

Gravity-Gradient Noise Mitigation via Deep Learning for the Einstein Telescope

David Bertram,* Markus Bachlechner and Achim Stahl

*Physics Institute IIIB, RWTH Aachen University,
Otto-Blumenthal-Straße 16, 52074 Aachen, Germany*

E-mail: david.bertram@rwth-aachen.de, mbachlechner@physik.rwth-aachen.de

As the first gravitational wave observatory of the third generation, the future Einstein Telescope (ET) aims to improve current sensitivities by at least one order of magnitude over the whole detection band. Specifically, in the low-frequency band below 10 Hz, gravity-gradient noise caused by seismic perturbations is anticipated to be the limiting noise contribution.

Therefore, the underground construction and additional mitigation will be critical for ET to achieve design sensitivity. The associated challenge is a precise reconstruction of gravity-gradient noise based on the activity recorded by an array of auxiliary seismic sensors.

We present a first proof-of-concept for a model-independent deep learning approach based on a stochastic seismic simulation and analytical gravity-gradient noise model. In addition, cancellation performance and sensor noise robustness tests for a spatiotemporal ResNet architecture are discussed, along with the potential for sensor array optimization.

*The European Physical Society Conference on High Energy Physics (EPS-HEP2023)
21-25 August 2023
Hamburg, Germany*

*Speaker

1. Introduction

Gravity-gradient noise (GGN) caused by seismic perturbations is anticipated to be the limiting factor for the sensitivity of third-generation gravitational wave detectors at frequencies below 10 Hz. For the future Einstein Telescope (ET), the foreseen underground construction alone will not provide sufficient shielding, and additional cancellation techniques based on auxiliary seismic sensors will be critical to achieving the design sensitivity. [1–3]

The success of such an approach is crucially dependent on a precise reconstruction of GGN based on the recordings of the underlying seismic activity. Since this task is equivalent to approximating a non-linear transfer function between a high dimensional input space with spatial as well as temporal features and the corresponding time-series of GGN, we propose the use of deep neural networks as depicted in Fig. 1.

This approach offers potential advantages over current alternatives, such as linear Wiener Filters [4]. On one hand, it ensures model independence by autonomously learning correlation factors. On the other hand, it offers the prospect of good

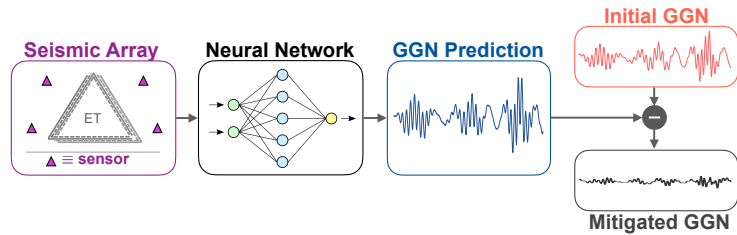


Figure 1: The proposed deep learning approach for GGN mitigation.

robustness against instrumental self-noise. This paper presents the first proof of concept for the above-mentioned approach based on a stochastic simulation of seismic activity and the modeling of the corresponding GGN. Further, performance tests for a spatiotemporal ResNet [5] architecture are presented along with an investigation of the potential for sensor array optimization.

2. Methodology & Simulation

Investigating the feasibility and potential of the proposed GGN mitigation technique requires seismic activity data as input to the network and the corresponding GGN as true labels. Until such data is available, either from R&D test facilities like ETpathfinder [6] or ultimately from ET measurements with GGN as the dominant noise contribution, testing and development must rely on simulated datasets. Therefore, we implemented a fast analytical simulation tool that exploits suited simplifications of the problem to obtain an adequate scenario for initial testing.

Seismic Field Simulation The seismic activity was simulated in a Monte-Carlo manner, i.e. through the stochastic sampling of multiple seismic pulses that propagate either as longitudinal p-wave or transversal s-wave modes through a homogenous half-space and together construct the seismic field. All relevant sampling or geological parameters were chosen to mimic Euregio Meuse-Rhine (EMR) candidate site conditions, resulting in very good agreement with the GGN estimate from the site characterization study [2].

The Seismometer Signals (Network Input) Seismic activity recorded by a sensor array is used as input for the GGN prediction. Starting from the simulated seismic fields, the signals are generated by superimposing the displacement waveforms with simulated instrumental self-noise. The latter is generated by coloring white noise with the known noise spectrum of state-of-the-art borehole

seismometers [7]. With such seismometers, high-precision measurements with a signal-to-noise ratio (SNR) on the order of 10^3 should be achievable at the EMR site in principle. [2, 7] However, an additional scenario with an SNR of $O(10)$ is implemented to test the noise robustness of the deep learning approach. Since there is no general concept for the positioning of seismometers yet, a regular 8×8 grid in the plane of the ET interferometers with a seismometer spacing of 3 km is chosen for our first test scenario. However, for follow-up studies, the use of optimized sensor arrays that reduce drilling costs, e.g., by exploiting the ET cavities, should be investigated.

GGN Strain (Network Labels) The GGN strain in the ET interferometers was finally derived from the simulated seismic field by modeling a simplified transfer function. Following Harms [8], the gravitational acceleration was approximated for test masses located at the center of spherical cavities as

$$\delta \vec{a}^{p/s}(\vec{r}_m, t) = \kappa^{p/s} G \rho_0 \vec{\xi}^{p/s}(\vec{r}_m, t) \frac{j_1(k^{p/s} a)}{k^{p/s} a} \quad (1)$$

where $\vec{\xi}^{p/s}(\vec{r}_m, t)$ is the simulated seismic displacement field evaluated at the position of the test masses. Further, $\kappa^p = 8\pi$ and $\kappa^s = -4\pi$ denote the coupling factors for longitudinal p-waves (bulk medium) and transversal s-waves (cavity surface), respectively. The gravitational constant is G , ρ_0 is the density of the homogeneous half-space, and $j_1(k^{p/s} a)$ is the first spherical Bessel function, depending on the product of wavenumber $k^{p/s}$ and cavity radius a . Finally, the GGN strain in the interferometers is determined by simplifying each mirror suspension as a single-stage pendulum and combining the displacements of the end and beam splitter mirrors.

3. Network Architecture & Noise Mitigation Performance

We treat the mapping of the transfer function between the seismic sensor array and the corresponding GGN as a multivariate time series regression task. The network learns to extract abstract spatial and temporal features from the seismic recordings and translate them into the corresponding GGN series. The architecture designed for this purpose is shown in Fig. 2.

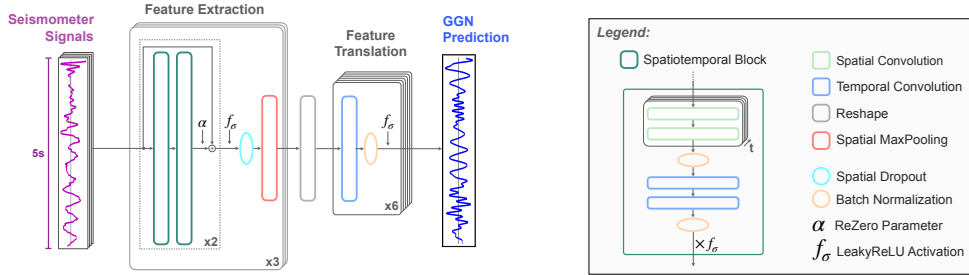


Figure 2: The spatiotemporal ResNet architecture for GGN prediction. A combination of spatial and temporal convolutional layers embedded in spatio-temporal ReZero blocks [9] (dark-green) is used to extract increasingly abstract features from the sensor array data. MaxPooling [10] (red) is used to reduce interim spatial dimensions and improve the learning of latent representations. The spatial convolutions (light-green) are time-distributed regular convolutions that can be exchanged for Graph convolutions [11] in case of irregular geometries. Along the time axis, WaveNet [12] inspired dilated temporal convolutions (blue) are applied. An exponentially increasing dilation factor is used to achieve a large receptive field. The same temporal layers are applied to finally translate the abstract series of interim features into the GGN prediction.

The network was trained to predict the GGN strain time series of 4×10^4 independent events, each caused by 5 seconds of seismic activity. Testing is performed for another 5×10^3 separate events and an exemplary waveform is presented below in Fig. 3.

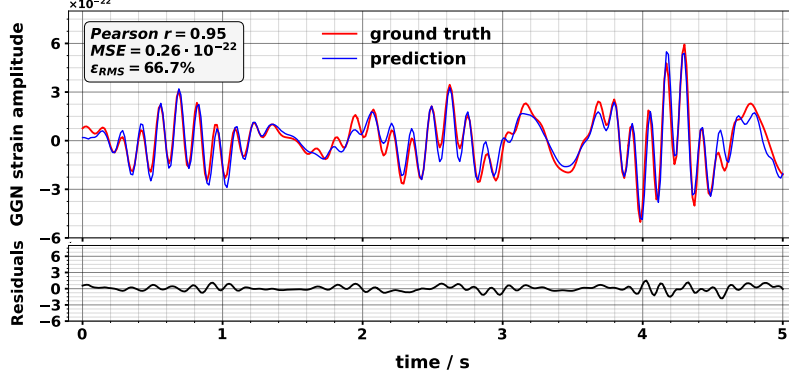


Figure 3: Exemplary display of a predicted GGN waveform (*blue*) compared to the simulated ground truth (*red*) in the top frame. The residuals after cancellation (*black*) are shown in the bottom frame.

Quantitative performance evaluation was performed by introducing two additional metrics to the mean square error (MSE), which is also used in training. We computed the Pearson correlation coefficient r_{xy} to measure the linear correlation between the predicted (y) and the ground truth (x) GGN waveforms within the test set.

$$r_{xy} \equiv \frac{\sum_i (x_i - \bar{x})(y_i - \bar{y})}{\sqrt{\sum_i (x_i - \bar{x})^2 \sum_i (y_i - \bar{y})^2}} \in [-1, 1] \quad \epsilon_{\text{RMS}} \equiv \frac{\text{RMS}(x) - \text{RMS}(x - y)}{\text{RMS}(x)} \quad (2)$$

Furthermore, the relative cancellation efficiency ϵ_{RMS} expresses the mitigation efficiency in terms of the root mean square (RMS) of the GGN before and after extinction relative to the original noise level. An evaluation of these metrics over the independent test set is shown in Fig. 4.

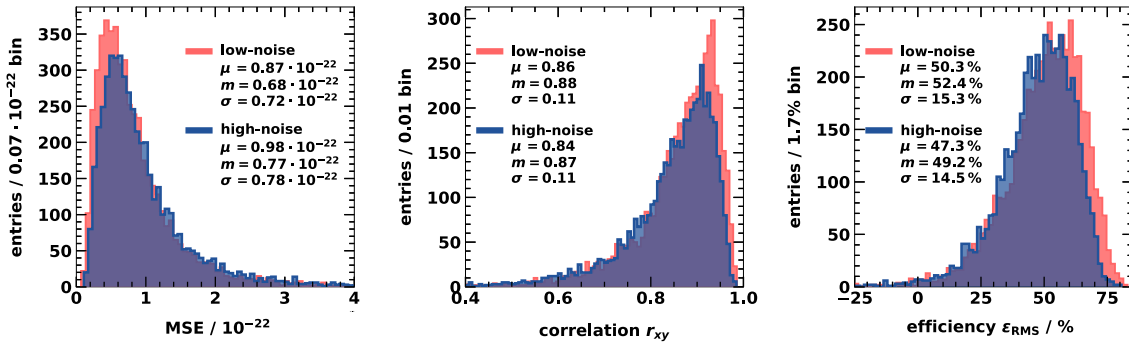


Figure 4: Evaluation of GGN mitigation performance. A comparison is shown for two instrumental self-noise scenarios: In the *red* scenario, the seismic sensors have a low, but in principle achievable, self-noise level of $\text{SNR} = \mathcal{O}(10^3)$. In *blue*, a significantly larger self-noise level of $\text{SNR} = \mathcal{O}(10)$ is considered for the input data of the network. In addition, the mean (μ), median (m) and standard deviation (σ) of each distribution are displayed.

Overall, the low MSE and high linear correlation coefficient demonstrate the ability of the network to correctly capture the complex transfer function between the seismic field recorded by

a sensor array and the GGN strain present in the ET interferometers. This is underlined by an average two-fold mitigation, as indicated by the ϵ_{RMS} histograms. The circumstance that a much higher instrumental noise scenario is only accompanied by minor losses in mitigation performance suggests the robustness of the deep learning approach to instrumental sensor noise.

4. Towards Optimized Seismic Sensor Arrays

A general challenge for GGN mitigation at ET is the positioning of the seismic sensor array. The goal is to reduce drilling costs while maintaining the highest possible GGN correlation. As a first step towards deep learning optimized sensor arrays, we analyzed the relative importance of each sensor in the array based on the idea that important sensors have large gradients [13].

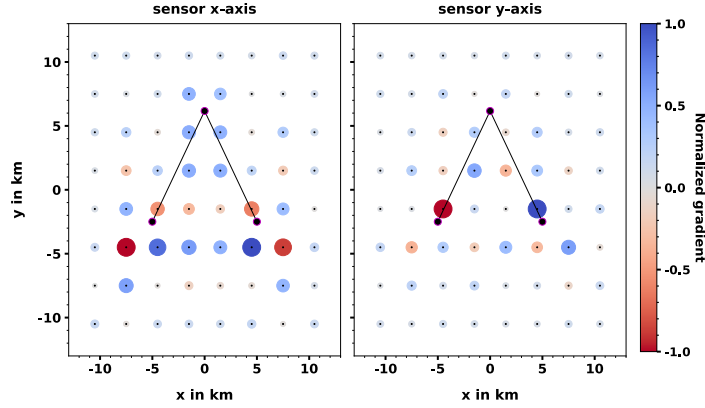


Figure 5: Relative sensor importance analysis. The saliency maps of the sensor’s x-axis and y-axis are shown on the left and right respectively. The size and color of each dot represent the absolute value and sign of the gradients of each seismic sensor during GGN prediction. The ET interferometer is drawn in black.

The results in Fig. 5 show that the sensors in the vicinity of the ET end mirrors are of dominant importance due to the greater spatiotemporal correlation and effect on the strain signal. Further, both sensor axes show symmetry patterns around the beam-splitter mirrors at $x = 0$. A mirror symmetry for the x-axis and anti-correlation for the y-axis indicates that the network internalizes the geometrical properties of the working principle of the interferometer. The primary motivation behind this is to demonstrate the potential of using neural networks to gain insight into key sensor locations and potentially usable symmetries, and ultimately bridge to a seismic sensor array with optimized efficiency.

5. Conclusion

Cancellation of GGN by a factor of two to three will be critical for achieving ET design sensitivity. [1, 3] We presented a successful proof-of-concept for a deep learning based approach with two-fold cancellation and good instrumental self-noise robustness. To further test the capabilities of this method, more refined simulations with more realistic geologies and GGN models, or real data from R&D prototypes should be used. The main challenge will be unbiased learning from data that may vary over several orders of magnitude, with potentially strong underlying frequency distributions resulting from seismic site characteristics. Next steps include the optimization of the sensor array and adapting the network to operate on irregular grids encoded in graph structures.

References

- [1] ET Steering Committee Editorial Team (2020), *Design Report Update for the Einstein Telescope*, [ET-007B-20](#).
- [2] M. Bader, S. Koley, J. Van Den Brand, et al (2022), *Newtonian-noise Characterization at Terziet in Limburg the Euregio Meuse–Rhine Candidate Site for Einstein Telescope*, *Class. Quantum Grav.* **39** 025009 [doi:10.1088/1361-6382/ac1be4].
- [3] J. Harms, L. Naticchioni, E. Calloni, et al. (2022), *A Lower Limit for Newtonian-Noise Models of the Einstein Telescope*, *Eur. Phys. J. Plus* **137** 687 [doi:10.1140/epjp/s13360-022-02851-z].
- [4] M. Coughlin, N. Mukund, J. Harms, et al. (2016), *Towards a First Design of a Newtonian-Noise Cancellation System for Advanced LIGO*, *Class. Quantum Grav.* **33** 244001 [doi:10.1088/0264-9381/33/24/244001].
- [5] K. He, X. Zhang, S. Ren and J. Sun (2016), *Deep Residual Learning for Image Recognition*, [arXiv:1512.03385](#) (Computer Vision and Pattern Recognition) [cs.CV/1512.03385].
- [6] A. Utina, A. Amato, J. Arends, et al. (2022), *ETpathfinder: a Cryogenic Testbed for Interferometric Gravitational-Wave Detectors*, *Class. Quantum Grav.* **39** 215008 [doi:10.1088/1361-6382/ac8fdb].
- [7] B. Merchant and G. Slad for the Sandia National Laboratories (2017), *Next Generation Qualification: Kinematics STS-5A Seismometer Evaluation*, [SAND2017-11428 658005](#) [doi:10.2172/1405269].
- [8] J. Harms (2019), *Terrestrial Gravity Fluctuations*, *Living Rev. Relativ.* **22**, 6 [doi:10.1007/s41114-019-0022-2].
- [9] T. Bachlechner, B. Majumder, H.Mao et al. (2020), *ReZero is All You Need: Fast Convergence at Large Depth*, [arXiv:2003.04887v2](#) (Machine Learning, Computation and Language) [cs.LG/2003.04887v2].
- [10] A. Zafar, M. Aamir, N. Mohd Nawi, et al. (2022), *A Comparison of Pooling Methods for Convolutional Networks*, *Appl. Sci.* **12** 8643 [doi:10.3390/app12178643].
- [11] J. Zhou, C. Ganqu, H. Shengding, et al. (2020), *Graph Neural Networks: A Review of Methods and Applications*, *AI Open* **1** 57-81 [doi:10.1016/j.aiopen.2021.01.001].
- [12] A. van den Oord, S. Dieleman, H. Zen et, al. (2016), *WaveNet: A Generative Model for Raw Audio*, [arXiv:1609.03499](#) (Sound, Machine Learning) [cs.LG/1609.03499].
- [13] K. Simonyan, A. Vedaldi, A. Zisserman (2014), *Deep Inside Convolutional Networks: Visualising Image Classification Models and Saliency Maps* [arXiv:1312.6034](#) (Computer Vision and Pattern Recognition) [cs.CV/1312.6034].